Electronic Supplementary Material (ESI) for CrystEngComm.

Supplementary Material (ESI) for CrystEngComm

Polycarboxylates-directed pyridyl-amide-based Co^{II} complexes: fluorescent recognition of Fe^{3+} and Fe^{3+}-functionalized composite materials for enhancing photocatalytic activities

Ying Xiong, GuoCheng Liu*, XiuLi Wang*, JuWen Zhang, HongYan Lin and XiaoTing Sha

Table S1. (a) Selected bond distances (Å) and angles (°) for complex **1**

$C_{28}H_{30}CoN_4O_{10}$			
Co(1)–N(1)	2.163(3)	Co(1)–O(1W)	2.063(3)
Co(1)–N(1)#1	2.163(3)	Co(1) –O(1W)#1	2.063(3)
Co(1)–O(2)	2.056(2)	Co(1)–O(2) #1	2.056(2)
O(2)–Co(1)–O(2)#1	180.0	O(1W)#1–Co(1)–N(1)#1	90.49(13)
O(2)–Co(1)–O(1W)#1	90.95(10)	O(1W)–Co(1)–N(1)#1	89.51(13)
O(2)#1–Co(1)–O(1W)#1	89.05(10)	O(2)–Co(1)–N(1)	89.75(11)
O(2)–Co(1)–O(1W)	89.05(10)	O(2)#1–Co(1)–N(1)	90.25(11)
O(2)#1–Co(1)–O(1W)	90.95(10)	O(1W)#1–Co(1)–N(1)	89.51(13)
O(1W)#1–Co(1)–O(1W)	180.0	O(1W)–Co(1)–N(1)	90.49(13)
O(2)–Co(1)–N(1)#1	90.25(11)	N(1)#1–Co(1)–N(1)	180.0
O(2)#1–Co(1)–N(1)#1	89.75(11)		

Symmetry transformations used to generate equivalent atoms: #1 $-x + 1, -y, -z$.

Table S1. (b) Selected bond distances (Å) and angles (°) for complex **2**

$C_{34}H_{28}CoN_4O_8$			
Co(1)–O(4)#1	2.056(2)	Co(1)–N(1)	2.100(2)
Co(1)–N(3)	2.070(2)	Co(1)–O(5)#1	2.254(2)
Co(1)–O(1)	2.074(2)	Co(1)–O(2)	2.262(2)
O(4)#1–Co(1)–N(3)	102.75(9)	O(1)–Co(1)–O(5)#1	98.05(8)
O(4)#1–Co(1)–O(1)	149.84(9)	N(1)–Co(1)–O(5)#1	164.09(9)
N(3)–Co(1)–O(1)	96.64(10)	O(4)#1–Co(1)–O(2)	95.06(8)
O(4)#1–Co(1)–N(1)	103.46(9)	N(3)–Co(1)–O(2)	154.56(9)
N(3)–Co(1)–N(1)	100.28(10)	O(1)–Co(1)–O(2)	60.27(9)
O(1)–Co(1)–N(1)	95.44(10)	N(1)–Co(1)–O(2)	92.95(9)
O(4)#1–Co(1)–O(5)#1	60.82(8)	O(5)#1–Co(1)–O(2)	86.48(8)
N(3)–Co(1)–O(5)#1	86.52(9)		

Symmetry transformations used to generate equivalent atoms: #1 $x, y + 1, z$.

Table S1. (c) Selected bond distances (Å) and angles (°) for complex **3**

$C_{34}H_{28}CoN_4O_7$			
Co(1)–O(3)#1	2.076(3)	Co(1)–O(4)#2	2.133(3)
Co(1)–O(2)#1	2.091(2)	Co(1)–N(1)	2.168(3)
Co(1)–O(1)	2.117(3)	Co(1)–N(4)#3	2.181(3)
O(3)#1–Co(1)–O(2)#1	94.86(10)	O(3)#1–Co(1)–O(1)	175.04(10)
O(2)#1–Co(1)–O(1)	90.06(10)	O(3)#1–Co(1)–O(4)#2	88.02(10)
O(2)#1–Co(1)–O(4)#2	176.32(10)	O(1)–Co(1)–O(4)#2	87.10(10)
O(3)#1–Co(1)–N(1)	87.91(11)	O(2)#1–Co(1)–N(1)	96.10(11)
O(1)–Co(1)–N(1)	92.28(11)	O(4)#2–Co(1)–N(1)	81.70(11)
O(3)#1–Co(1)–N(4)#3	97.05(11)	O(2)#1–Co(1)–N(4)#3	88.40(11)
O(1)–Co(1)–N(4)#3	82.36(11)	O(4)#2–Co(1)–N(4)#3	93.53(12)
N(1)–Co(1)–N(4)#3	173.03(12)		

Symmetry transformations used to generate equivalent atoms: #1 $-x + 1, -y, -z + 1$; #2 $x - 1, y, z$; #3 $x, y, z - 1$.

Table S1. (d) Selected bond distances (Å) and angles (°) for complex **4**

$C_{28}H_{25}CoN_5O_{10}$			
Co(1)–O(1)	1.970(2)	Co(1)–O(6)#1	1.997(2)
Co(1)–N(4)#2	2.042(2)	Co(1)–N(1)	2.049(2)
O(1)–Co(1)–O(6)#1	97.48(8)	O(1)–Co(1)–N(4)#2	113.15(9)
O(6)#1–Co(1)–N(4)#2	102.20(9)	O(1)–Co(1)–N(1)	113.90(9)
O(6)#1–Co(1)–N(1)	111.93(9)	N(4)#2–Co(1)–N(1)	115.94(9)

Symmetry transformations used to generate equivalent atoms: #1 $x + 1, y, z$, #2 $-x - 1, -y - 1, -z$.

Table S1. (e) Selected bond distances (Å) and angles (°) for complex **5**

$C_{18}H_{14}CoN_3O_6$			
Co(1)–O(3)#1	2.0223(17)	Co(1)–O(4)#2	2.0374(17)
Co(1)–O(2)	2.1530(17)	Co(1)–N(1)	2.163(2)
Co(1)–O(1)	2.2084(17)	Co(1)–N(3)#3	2.246(2)
O(3)#1–Co(1)–O(4)#2	106.67(7)	O(3)#1–Co(1)–O(2)	155.43(7)
O(4)#2–Co(1)–O(2)	96.05(7)	O(3)#1–Co(1)–N(1)	98.67(8)
O(4)#2–Co(1)–N(1)	89.04(8)	O(3)#1–Co(1)–O(1)	96.68(7)
O(2)–Co(1)–N(1)	90.80(7)	O(4)#2–Co(1)–O(1)	156.24(7)
O(2)–Co(1)–O(1)	60.20(6)	N(1)–Co(1)–O(1)	91.76(7)
O(3)#1–Co(1)–N(3)#3	86.41(8)	O(4)#2–Co(1)–N(3)#3	83.23(7)
O(2)–Co(1)–N(3)#3	87.11(7)	N(1)–Co(1)–N(3)#3	171.73(8)
O(1)–Co(1)–N(3)#3	94.15(7)		

Symmetry transformations used to generate equivalent atoms: #1 $x, y + 1, z$; #2 $-x + 1, -y, -z + 2$;

#3 – *x* + 2, –*y*, –*z* + 2.

Table S1. (f) Selected bond distances (Å) and angles (°) for complex **6**

$C_{78}H_{74}Co_3N_{12}O_{26}$			
Co(1)–O(1)#1	2.0420(16)	Co(1)–O(1)	2.0420(16)
Co(1)–O(2W)	2.1495(17)	Co(1)–N(1)#1	2.192(2)
Co(1)–O(2W)#1	2.1496(17)	Co(1)–N(1)	2.192(2)
Co(2)–O(1W)	2.087(2)	Co(2)–O(3)	2.0352(16)
Co(2)–N(9)	2.158(2)	Co(2)–N(3)	2.160(2)
Co(2)–O(5)#2	2.1770(17)	Co(2)–O(6)#2	2.3057(18)
O(1)#1–Co(1)–O(1)	179.999(2)	O(1)#1–Co(1)–O(2W)	90.78(7)
O(1)–Co(1)–O(2W)	89.22(7)	O(1)#1–Co(1)–O(2W)#1	89.22(7)
O(1)–Co(1)–O(2W)#1	90.78(7)	O(2W)–Co(1)–O(2W)#1	180.0
O(1)#1–Co(1)–N(1)#1	92.08(7)	O(1)–Co(1)–N(1)#1	87.92(7)
O(2W)–Co(1)–N(1)#1	86.77(7)	O(2W)#1–Co(1)–N(1)#1	93.24(7)
O(1)#1–Co(1)–N(1)	87.92(7)	O(1)–Co(1)–N(1)	92.08(7)
O(2W)–Co(1)–N(1)	93.24(7)	O(2W)#1–Co(1)–N(1)	86.76(7)
N(1)#1–Co(1)–N(1)	180.0	O(3)–Co(2)–O(1W)	89.74(8)
O(3)–Co(2)–N(9)	116.55(7)	O(1W)–Co(2)–N(9)	89.93(9)
O(3)–Co(2)–N(3)	93.39(8)	O(1W)–Co(2)–N(3)	174.84(8)
N(9)–Co(2)–N(3)	92.33(8)	O(3)–Co(2)–O(5)#2	151.38(7)
O(1W)–Co(2)–O(5)#2	83.43(7)	N(9)–Co(2)–O(5)#2	91.29(7)
N(3)–Co(2)–O(5)#2	91.88(7)	O(3)–Co(2)–O(6)#2	93.96(7)
O(1W)–Co(2)–O(6)#2	89.14(8)	N(9)–Co(2)–O(6)#2	149.47(7)
N(3)–Co(2)–O(6)#2	86.55(8)	O(5)#2–Co(2)–O(6)#2	58.30(6)

Symmetry transformations used to generate equivalent atoms: #1 –*x* – 1,–*y* + 1,–*z* + 1; #2 *x* + 1, *y*, *z*.

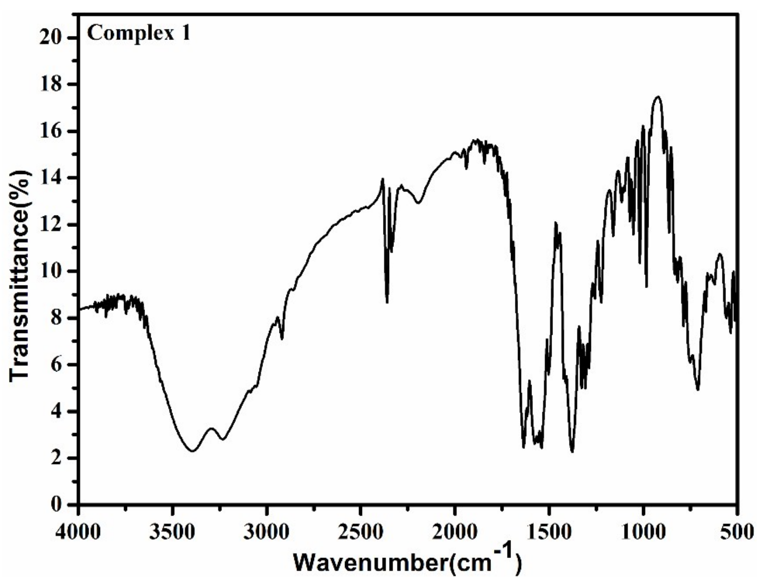

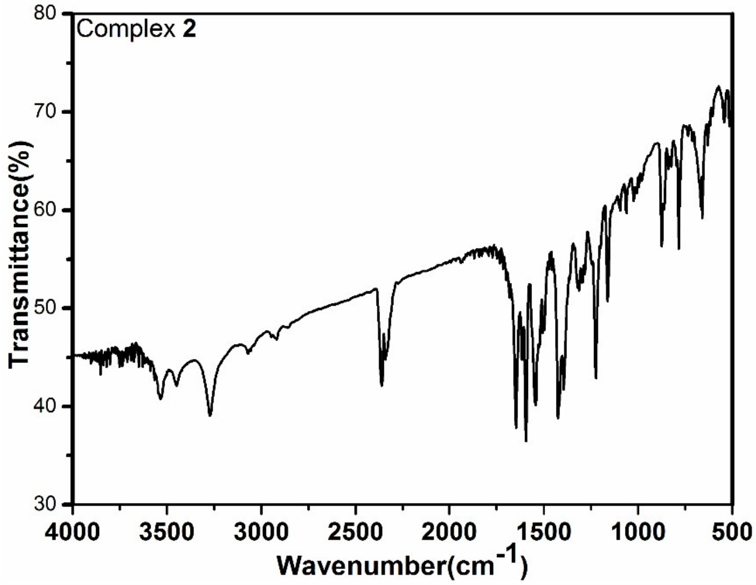
Complex 2
Transmittance(%)
Wavenumber(cm-1)
80
70
60
50
40
30
4000
3500
3000
2500
2000
1500
1000
500

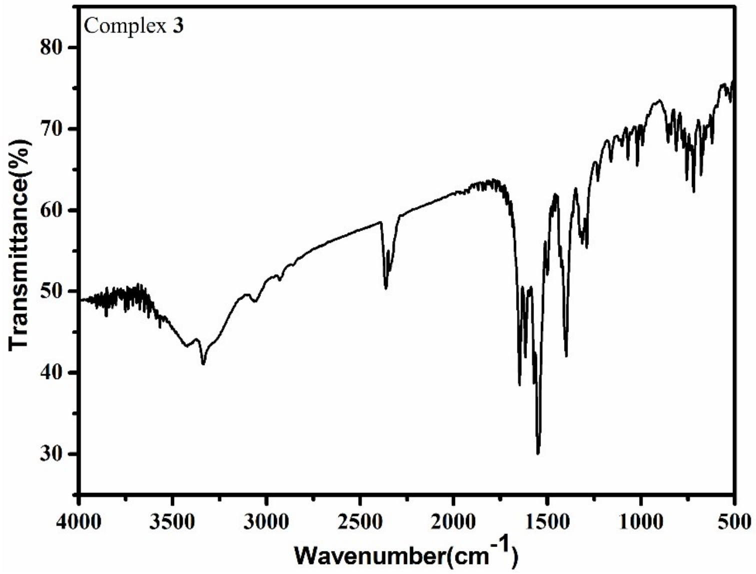
Complex 3
Transmittance(%)
Wavenumber(cm-1)
80
70
60
50
40
30
4000
3500
3000
2500
2000
1500
1000
500

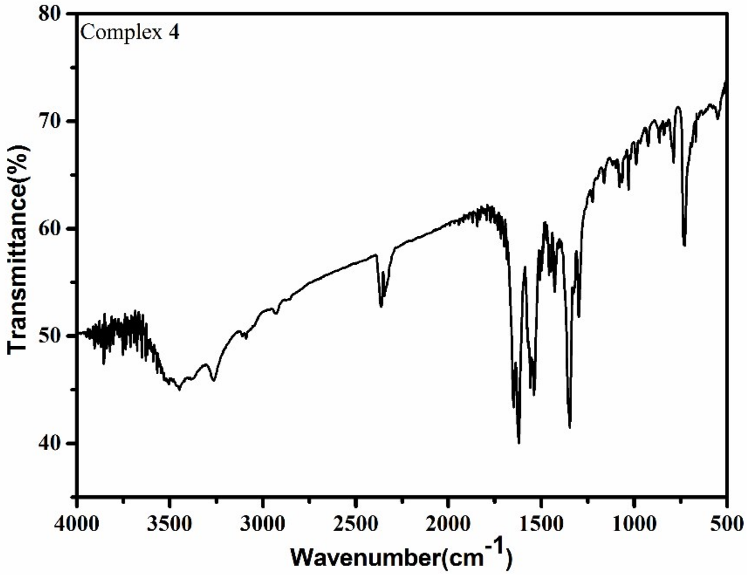
Complex 4
Transmittance(%)
Wavenumber(cm-1)
80
70
60
50
40
4000
3500
3000
2500
2000
1500
1000
500

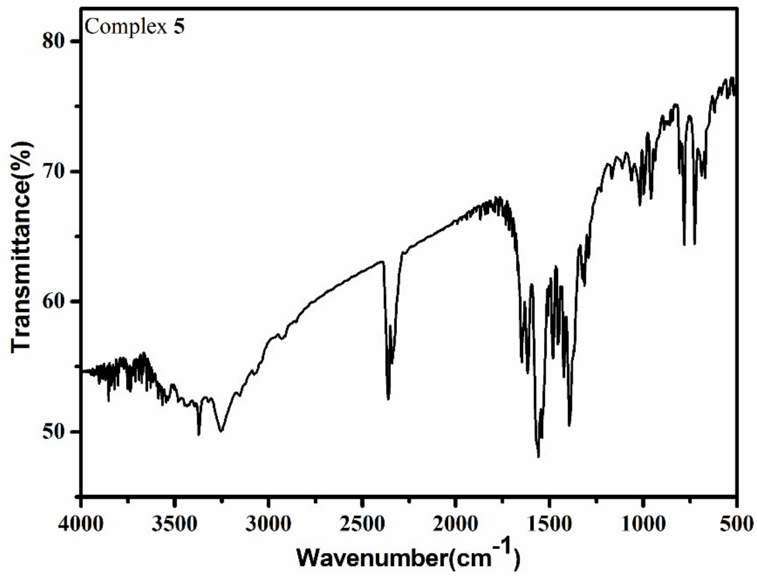

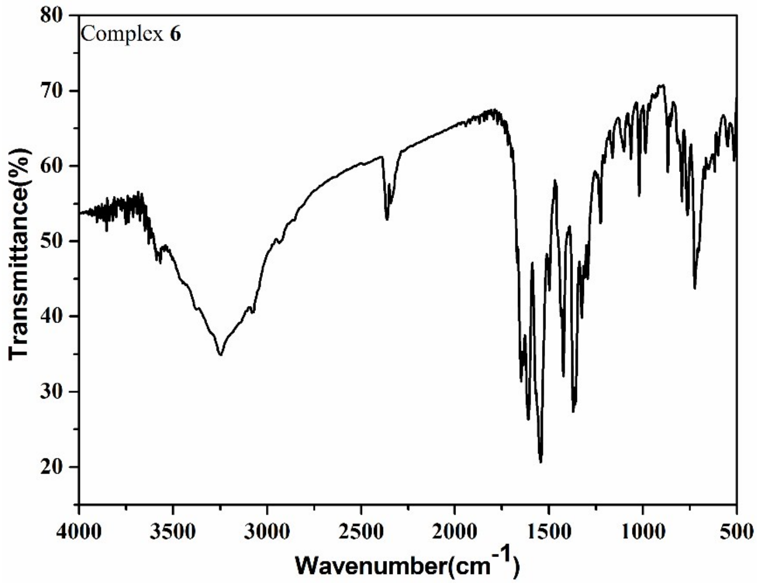

Fig. S1. The IR spectra of complexes **1–6**.

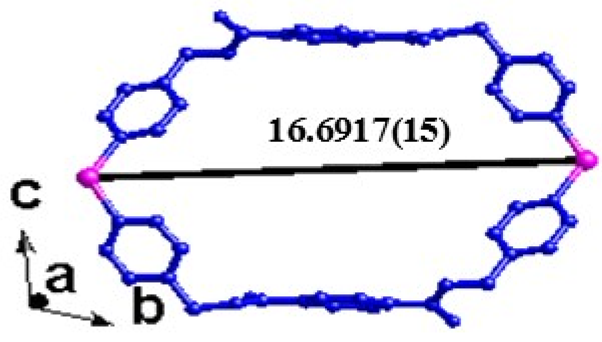

Fig. S2. The 38-membered $[Co_2(4\text{-bmbpd})]_2$ loop of **4**.

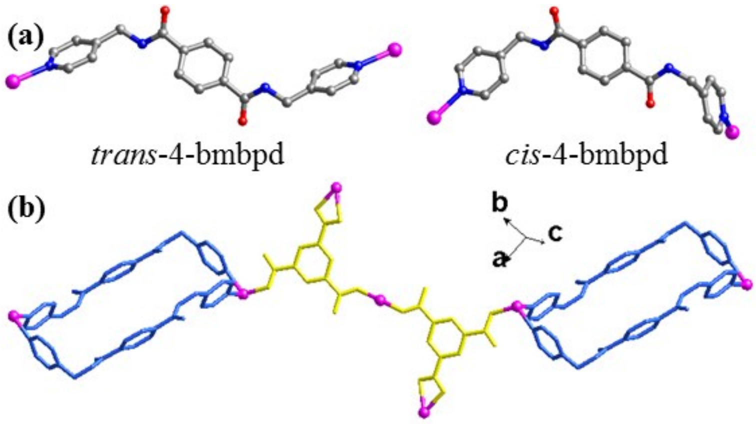

Fig. S3. (a) The coordination modes of the *trans*- and *cis*-4-bmbpd ligand in **6**. (b) The 1D chain in **6**.

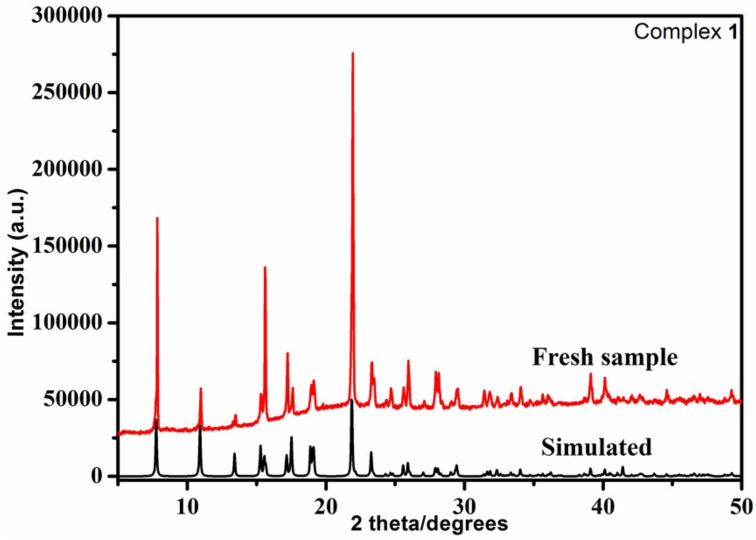

(a)

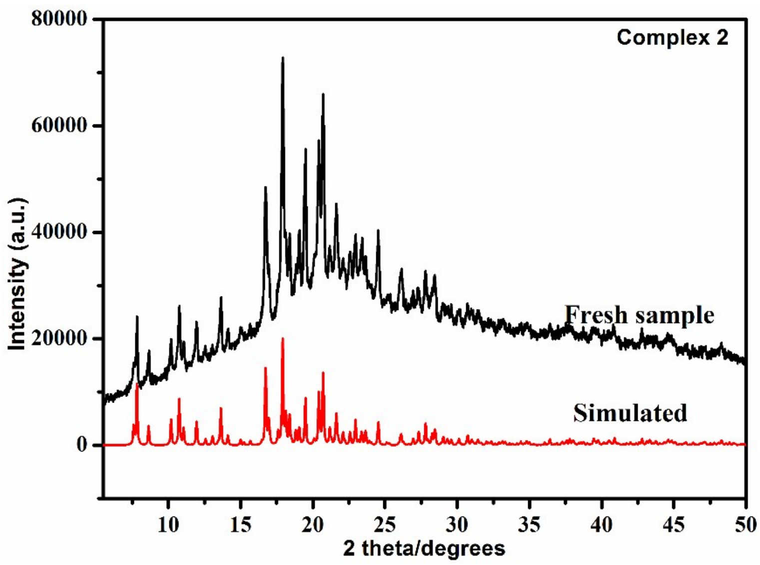

(b)

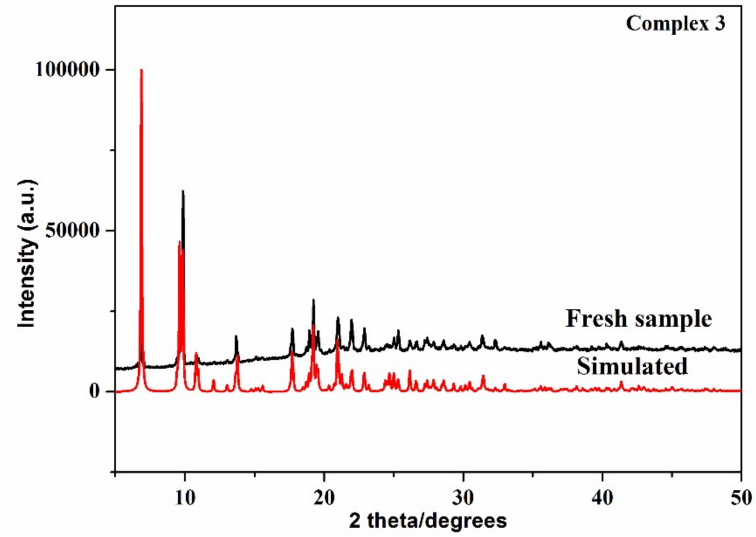
Complex 3
100000
50000
0
Intensity (a.u.)
Fresh sample
Simulated
10
20
30
40
50
2 theta/degrees

(c)

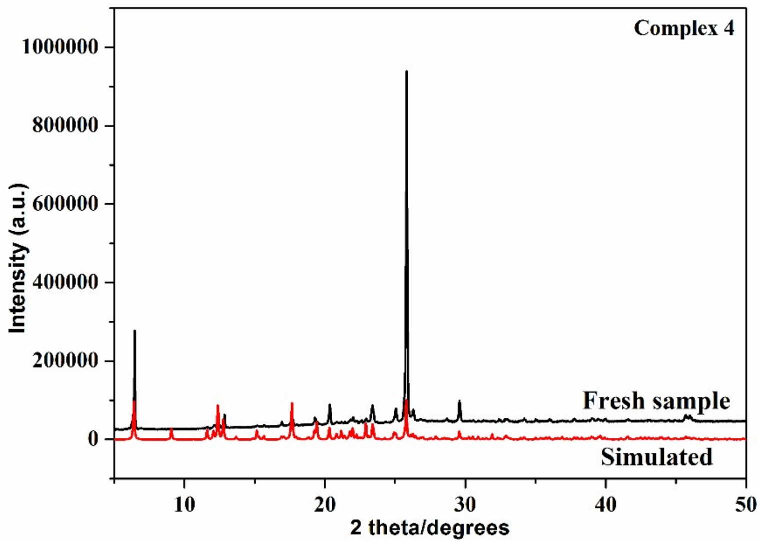
Complex 4
1000000
800000
600000
400000
200000
0
Intensity (a.u.)
Fresh sample
Simulated
10
20
30
40
50
2 theta/degrees

(d)

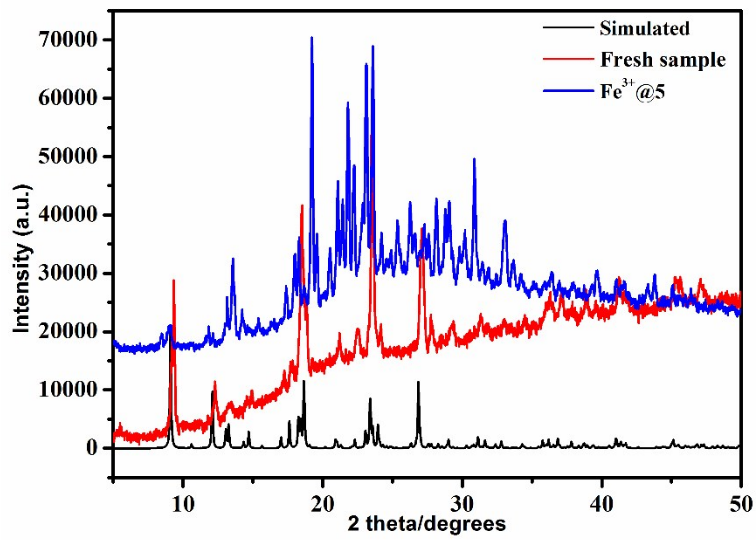
Simulated
Fresh sample
Fe^{3+}@5
70000
60000
50000
40000
30000
20000
10000
0
Intensity (a.u.)
10
20
30
40
50
2 theta/degrees

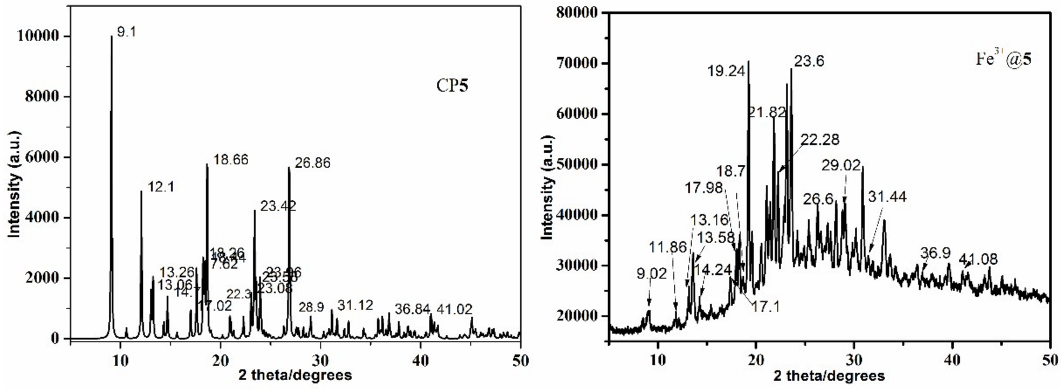

(e)

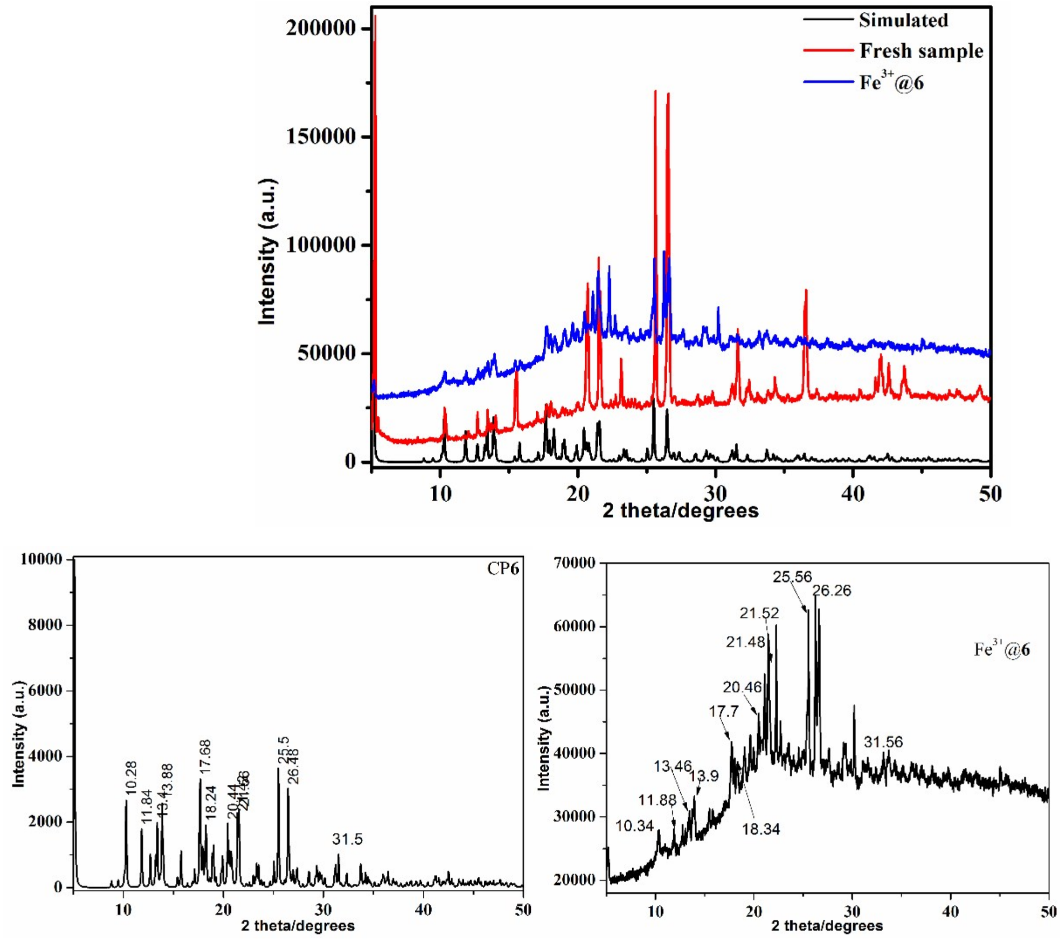

(f)

Fig. S4. The PXRD patterns of complexes **1–6** and the PXRD of Fe^{3+}@**5** and Fe^{3+}@**6**.

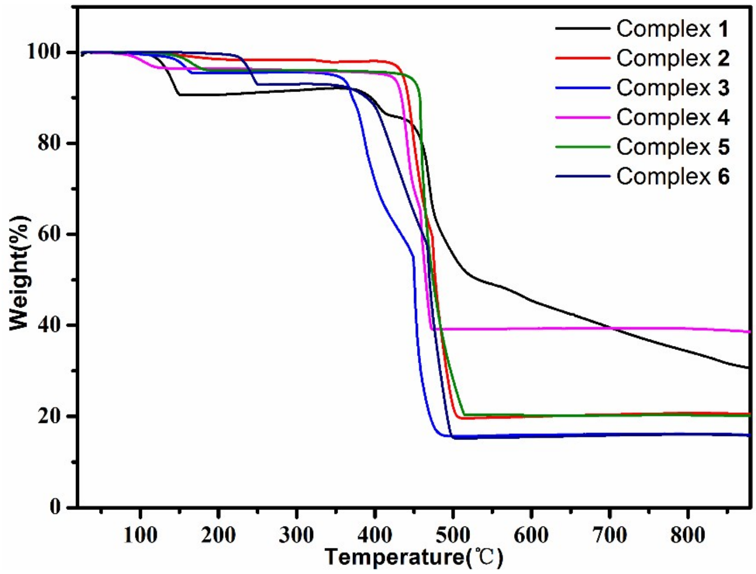

Fig. S5. The TG curves of complexes **1–6**.

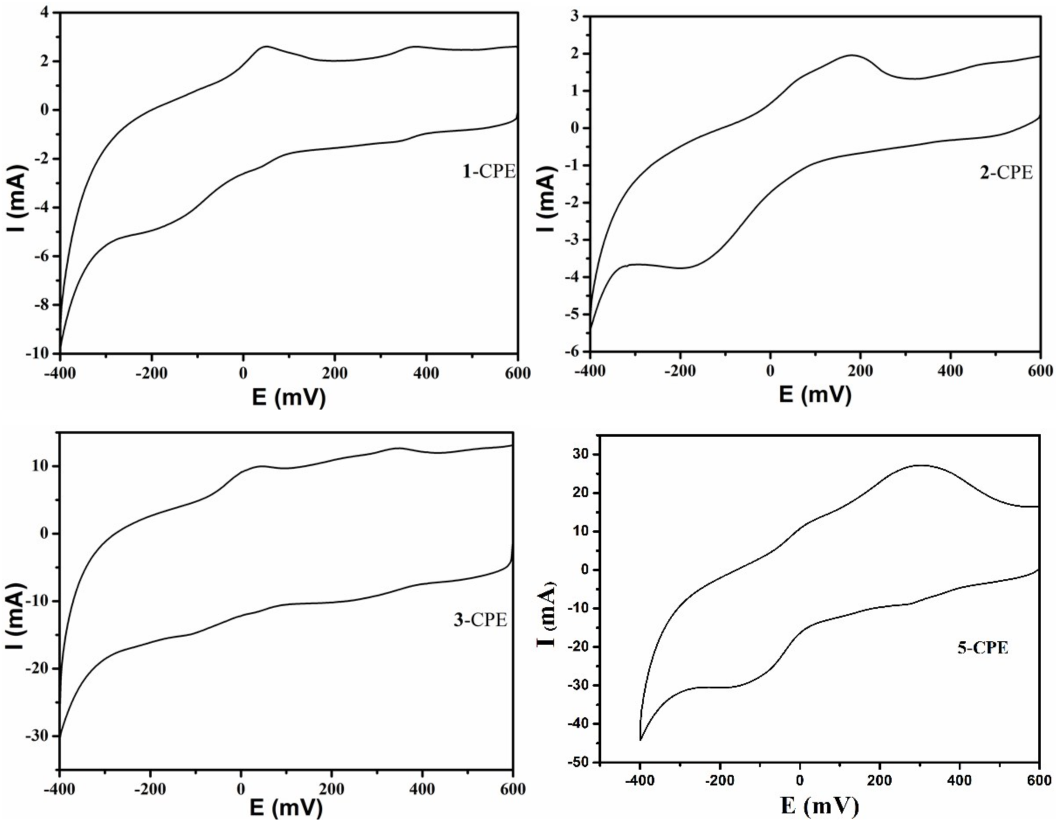

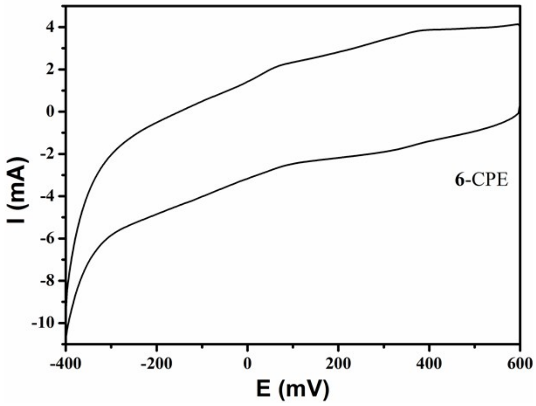

Fig. S6. Cyclic voltammograms of the **1**-, **2**-, **3**-, **5**-, **6**-CPE in the 0.01 M H_2SO_4 + 0.5 M Na_2SO_4 aqueous solution.

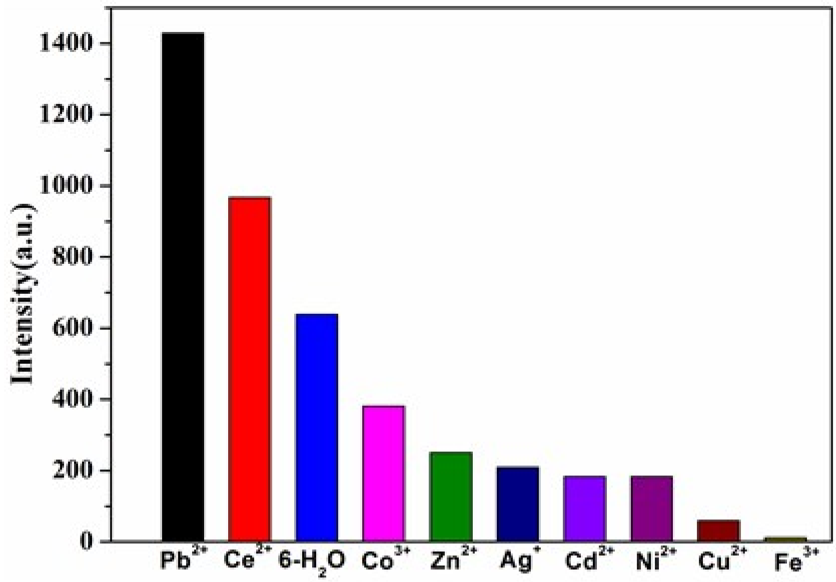

(a)

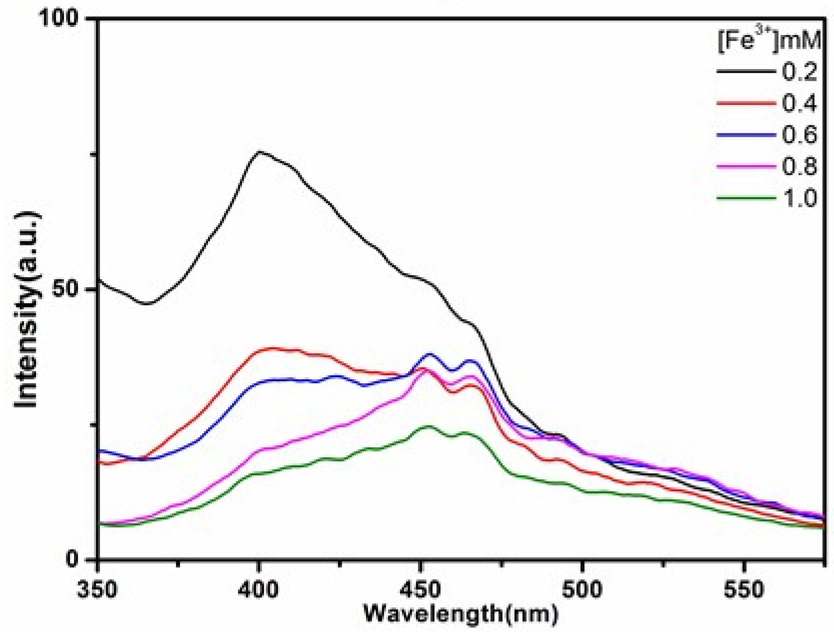

(b)

Fig. S7. (a) The relative luminescence intensities of M^{n+}@**6** in aqueous solutions. (b) Emission spectra of Fe^{3+}@**6** aqueous suspensions with the concentration of Fe^{3+} in the range 2×10^{-4}–1×10^{-3} M.

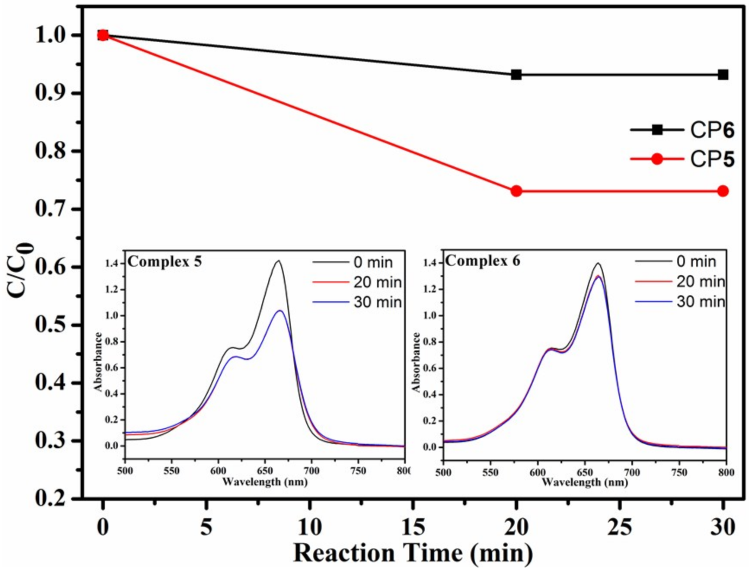

Fig.S8. The absorption spectra of the MB solution during the decomposition reaction without UV irradiation in the presence of CP**5** and CP**6.**

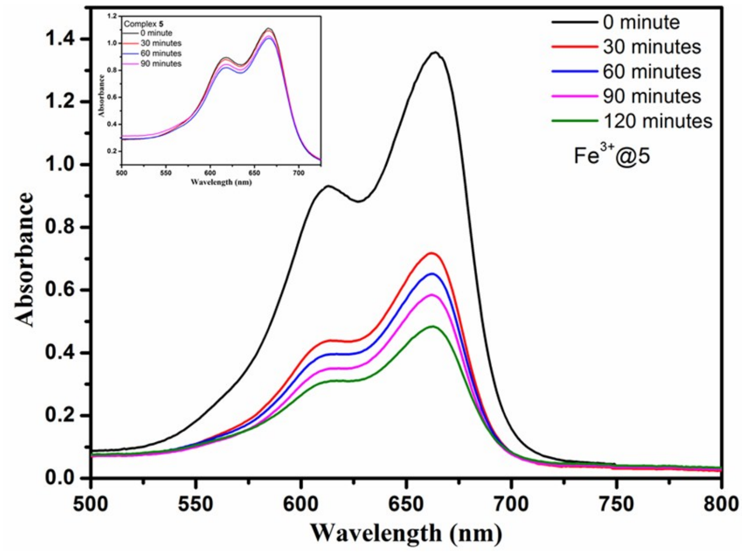

Fig. S9. Absorption spectra of the MB solution during the decomposition reaction under UV irradiation in the presence of Fe^{3+}@**5** and the inset is the absorption spectra of the MB solution during the decomposition reaction under UV irradiation in the presence of **5.**